BULLETIN OF THE POLISH ACADEMY OF SCIENCES
TECHNICAL SCIENCES, Vol. 63, No. 4, 2015
DOI: 10.1515/bpasts-2015-0097

Optimization of process parameters of friction stir welded AA 5083-O aluminum alloy using Response Surface Methodology

S. JANNET[1]*, P. KOSHY MATHEWS[2], and R. RAJA[1]

[1] Mechanical Department, Karunya University, Coimbatore-641114, Tamilnadu, India
[2] Kalaivani College of Technology, Coimbatore-641105, Tamilnadu, Coimbatore, India

Abstract. A methodology was exhibited to create the experimental model for assessing the Ultimate Tensile Strength of AA 5083-O aluminum compound which is broadly utilized as a part of boat building industry by Friction Stir Welding (FSW). FSW process parameters, such as: tool rotational speed, welding speed, and axial force were optimized for better results. FSW was completed considering three-component 3-level Box Behnekn Design. Response surface Methodology (RSM) was implemented to obtain the relationship between the FSW process parameters and ultimate Tensile Strength. Analysis of Variance (ANOVA) procedure was utilized to check the aptness of the created model. The FSW process parameters were additionally streamlined utilizing Response Surface Methodology (RSM) to augment tensile strength. The joint welded at a rotational speed of 1100 rpm, a welding speed of 75 mm/min and a pivotal energy of 2.5 t displays higher tensile strength compared with different joints in comparison with other joints.

Key words: friction stir welding, optimization, Response Surface Analysis, Analysis of Variance, tensile strength.

1. Introduction

Da Silva has investigated the effect of joining parameters on the mechanical properties, microstructural features and material flow of dissimilar aluminum alloy joints produced by friction stir welding [1]. Scialpi studied the friction stir welding of thin aluminum alloy of 0.8 mm thick. Fatigue behavior of spot friction welds or friction stir spot welds in lap-shear and cross-tension specimens of dissimilar aluminum 6 mm thick sheets were investigated. Basing on experimental observations and three fatigue life estimation models the effective stress intensity factor and J integral solutions at the critical locations of the welds obtained from three-dimensional finite element analyses appear to be apropriate. Fracture mechanics parameters to correlate the experimental fatigue data for the 5754/7075 and 7075/5754 welds in lap-shear and cross-tension specimens [2]. Bo Li, investigated the effects of the value of pin off-set, on weld formation, microstructures and mechanical tensile properties of the lap-butt joints of dissimilar aluminiums [3, 4]. C. Leitão studied the relation between weldability, material flow during FSW and the plastic behavior of the base materials, at different temperatures and found that the AA6082 alloy displays good weldability in FSW and AA 5083 alloy displayed poor weldability [5]. Koilraj analysed that defect free, high efficiency welded joints can be produced using a wide range of process parameters and recommends parameters for producing best joint tensile properties. Microstructural studies revealed that the material placed on the advancing side dominates the nugget region. Hardness studies showed that the lowest hardness in the weldment occurred in the heat-affected zone on alloy of 5083 side, where tensile failures were observed to take place [6]. Though various aluminum joints produced by FSW were studied by several researchers, optimization of the FSW process parameter for aluminum alloy AA5083-O which is used typically in the marine, automotive, structural and construction industries, has not yet been studied with help of response surface methodology (RSM). The RSM is helpful in developing a suitable ballpark figure for the well-designed relationship between the independent variables and the response variable that may exemplify the nature of the joints [7]. This has been proved by several researchers [8–11]. Tran Hung Tra showed that the fatigue crack propagation (FCP) rates were sensitive to the propagating location, the test temperature, and the PWHT condition as well [12]. It was also found that the different FCP rates were driven by the micro structural influences in and around the welded zone [12]. Hence, in this work, an attempt has been made to optimize the FSW process parameters to attain the maximum ultimate tensile strength for friction stir (FS) welded aluminum alloy AA 5083-O.

2. Experimental procedures

Aluminium 5083 is known for exceptional performance in extreme environments. 5083 is highly resistant to attack by both seawater and industrial chemical environments Alloy 5083 also retains exceptional strength after welding (Tables 1,2). It has the highest strength of the non-heat treatable alloys but is not recommended for use in temperatures in excess of 65°C FSW trials were carried out at 800, 1100 and 1400 rpm and for various transverse speeds ranging from 20 mm/min, 30 mm/min and 40 mm/min. It was observed that defect free joints could be observed all along the interface for specimen welded. The transverse cross section of the weld however displayed a slight tunneling defect at almost all runs.

*e-mail: sabithajannet@gmail.com

Table 1
Chemical composition of AA 5083-O

Element	Cr	Cu	Fe	Mg	Mn	Si	Ti	Zn	Al
AA 5083-O	0.05	0.10	0.40	4.90	0.40	0.40	0.15	0.25	Bal

Table 2
FSW process parameters and their levels

Parameter	Level		
	−1	0	1
Rotational speed (rpm)	800	1100	1400
Welding speed (mm/min)	25	50	75
Axial load (KN)	1.5	2	2.5

2.1. Selecting process parameters for FSW process. With a set of trial runs the independent process parameters affecting the ultimate tensile strength (UTS) were identified as tool rotational speed (N), welding speed(S), and axial force (F).

2.2. Manufacture of FSW tools. Tool made of high carbon high chromium steel has specifications of pin profile of straight square (SS) with shoulder diameter of 18 mm, pin diameter of 6 mm and pin length of 5.8 mm. The FSW tool was manufactured with CNC turning center and wire cut EDM machine to obtain an accurate profile. The manufactured tool is as shown in Fig. 1.

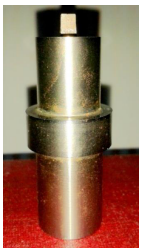

Fig. 1. Tool used for FSW

2.3. Development of design matrix. The selected design is shown in Table 3. It is a three factorial three level Box Behnken Design consisting of 15 sets of runs

Table 3
Design matrix and experimental value of UTS

Test No	Rotating Speed [rpm]	Welding Speed [mm/min]	Axial Load [F/t]	UTS [MPa]
1	−1	−1	0	266.8
2	1	−1	0	215.7
3	−1	1	0	219
4	1	1	0	220
5	−1	0	−1	229
6	1	0	−1	213
7	−1	0	1	249
8	1	0	1	230
9	0	−1	−1	210
10	0	1	−1	288.4
11	0	−1	1	266
12	0	1	1	230
13	0	0	0	245.3
14	0	0	0	270.4
15	0	0	0	214.2

2.4. Tensile test. In order to conduct the tensile test on the specimens, it has to be first cut according to the standard specifications (ASTM E08) as shown in Fig. 2. The distance between the jaws is increased beyond the length of the specimen by pressing the appropriate button in the control panel. Then the jaw is opened at both ends and the specimen is placed between the jaw and is tighten to keep the specimen rigidly fixed. Then the tensile load is applied gradually until it breaks. The required values and stress-strain diagram is obtained from the computer which uses the software WinUTM.

Fig. 2. Tensile test specimens

2.5. Development of mathematical model. Ultimate tensile strength of the FSW joints is function of rotational speed, welding speed and axial force and it can be expressed as

$$\mathrm{Y} = \mathrm{f}(\mathrm{N}, \mathrm{S}, \mathrm{F}).$$

For three factors the selected polynomial could be expressed as

$$\begin{aligned}\mathrm{UTS(MPa)} &= -29.33538 + 0.058769\mathrm{N} \\ &+ 0.076707\mathrm{F} - 3.11085\mathrm{E}{-}005\mathrm{NS} - 1.58316\mathrm{E}{-}005\mathrm{NF} \\ &+ 8.33153\mathrm{E}{-}004\mathrm{SF\text{-}2.03164E}{-}005\mathrm{N}^2 \\ &- 1.49088\mathrm{E}{-}003\mathrm{S}^2 - 1.28687\mathrm{E}{-}003\mathrm{F}^2.\end{aligned} \tag{1}$$

Table 4
Calculated regression coefficients of mathematical models

Factor	Calculated coefficient
Intercept	+274.93
A	+0.56
B	+3.04
C	+13.18
AB	+4.70
AC	−5.83
BC	+7.87
A^2	−35.24
B^2	−22.89
C^2	−11.52

2.6. Checking adequacy of model. The adequacy of the model developed was tested by using analysis of variance technique. The results of ANOVA are given in Table 6. The Model F-value of 9.05 implies that the model is significant. There is only a 1.29% chance that such a large F-value could occur due to noise. Values of "Prob > F" less than 0.0500 indicate model terms are significant. In this case C, A^2, B^2 are significant model terms. Values greater than 0.1000 indicate the model terms are not significant. If there are many insignificant model terms (not counting those required to support hierarchy), model reduction may improve your model. The "Lack of Fit F-value" of 0.53 implies the Lack of Fit is not significant relative to the pure error. There is a 70.53% chance that a "Lack of Fit F-value" this large could occur due to noise. Non-significant lack of fit is good we want the model to fit. The coefficient of determination R2 values gives the goodness of fitness of the model. The Predicted R-Squared of 0.5177 is not as close to the Adjusted R-Squared of 0.8381

Table 5
ANOVA Results

Source	Sum of Squares	df	Mean Square	F Value	p-value Prob > F	
Model	8238.05	9	915.34	9.05	0.0129	significant
A-Tool rotating speed	2.53	1	2.53	0.025	0.8805	
B-welding speed	73.81	1	73.81	0.73	0.4319	
C-axial load	1388.65	1	1388.65	13.73	0.0139	
AB	88.36	1	88.36	0.87	0.3928	
AC	135.72	1	135.72	1.34	0.2990	
BC	248.06	1	248.06	2.45	0.1781	
A^2	4585.75	1	4585.75	45.35	0.0011	
B^2	1934.87	1	1934.87	19.13	0.0072	
C^2	489.72	1	489.72	4.84	0.0790	
Residual	505.65	5	101.13			
Lack of Fit	223.94	3	74.65	0.53	0.7053	not significant
Pure Error	281.71	2	140.85			
Cor Total	8743.70	14				

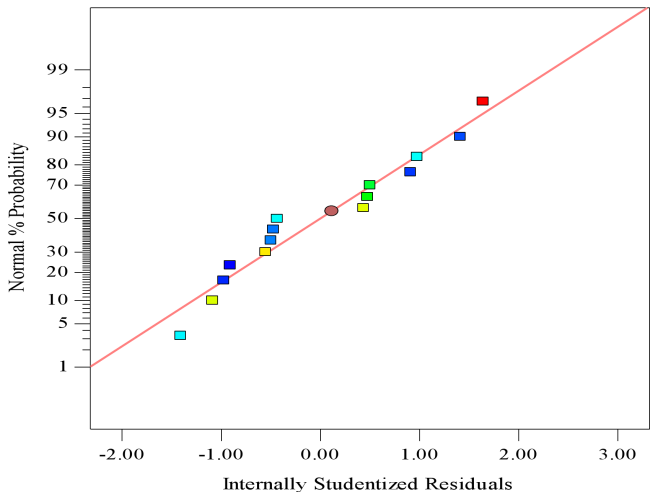

Fig. 3. Normal % probability plot

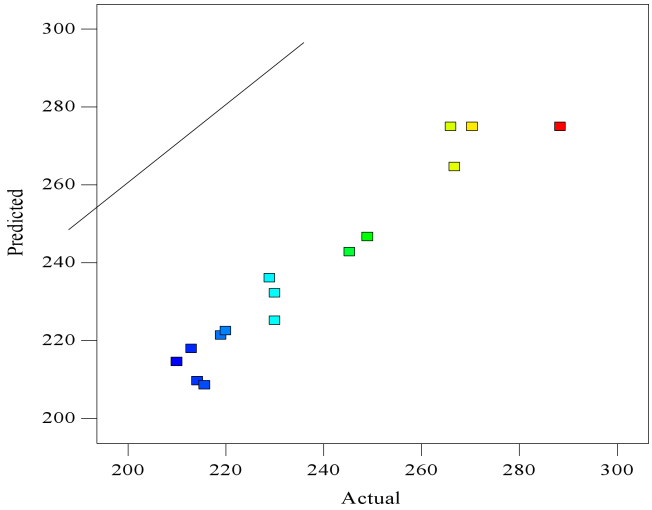

Fig. 4. Scatter diagram of ultimate tensile strength (UTS)

as one might normally expect. All empirical models should be tested by doing confirmation runs. A ratio greater than 4 is desirable [12]. Your ratio of 8.077 indicates an adequate signal. This model can be used to navigate the design space. The normal probability plot for tensile strength shown in Fig. 7 reveals that the residuals are falling on the straight line, which means the errors are distributed normally. A typical scatter diagram of the model is presented in Fig. 8. The observed values and predicted values of the responses are scattered close to the 45° line, indicating an almost perfect fit of the developed empirical models.

3. Effect of FSW process parameters

Ultimate tensile strength of FS welded aluminum alloy AA 5083-0 were predicted by the mathematical models using the experimental observations presented in Figs. 5 to 10, circumstances and end results. From Figs. 5 and 6, it is seen that as the rotational speed increases the tensile strength of FS welded AA 5083 increases and then decreases. It is clear that in FSW as the rotational speed increases, the heat generated increases. In the meantime, low rotational speed delivers low heat, which brings about the absence of stirring activity, thus the quality is low. From Figs. 5 and 10, it is evident that as welding speed increases from 30 mm/min to 108 mm/min, the tensile strength of the FS welded aluminum alloy AA 5083 increases and then decreases. At the lowest welding speed (30 mm/min) and highest welding speed (108 mm/min), lower tensile strength is observed. This is due to the increased frictional heat and insufficient frictional heat generated respectively [13]. From Figs. 7 and 1, it is observed that when the axial force increases from 0.8 to 1.8 t the ultimate tensile strength of the FS weld of AA 5083 increases and then decreases. This may be due to insufficient coalescence of transferred material. At the highest axial force, the plunge depth of the tool into the work pieces is higher, which results in lower tensile strength [14].

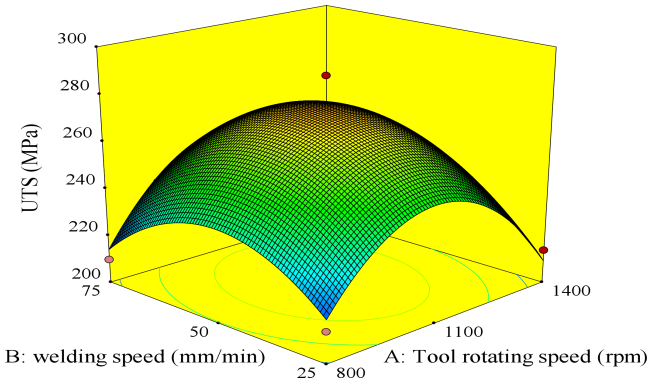

Fig. 5. Response surface graphs of tool rotational speed and welding speed on UTS

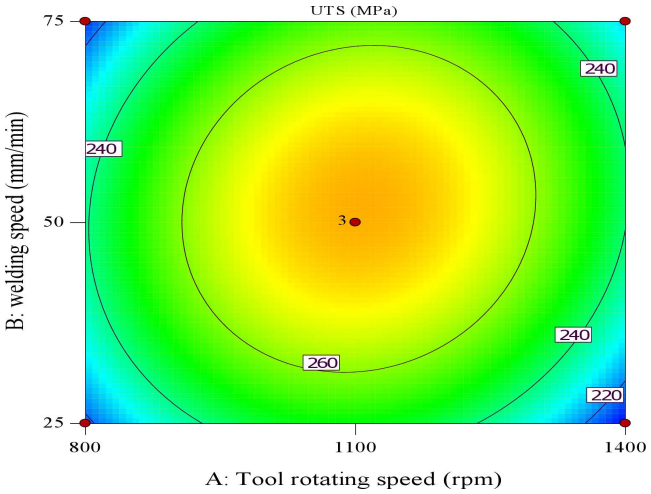

Fig. 6. Contour plots of tool rotational speed and welding speed on UTS

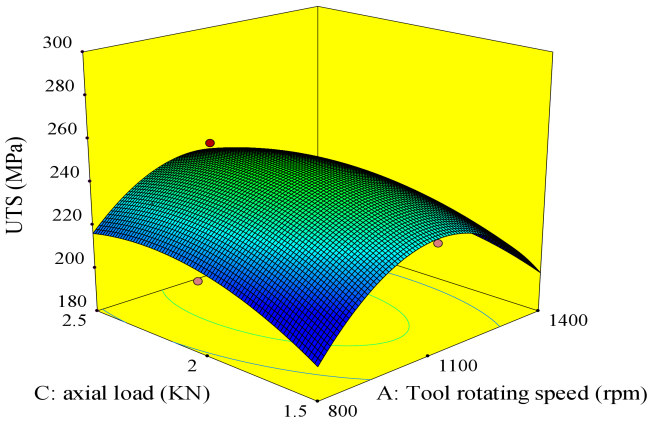

Fig. 7. Response surface graphs of tool rotational speed and axial load on UTS

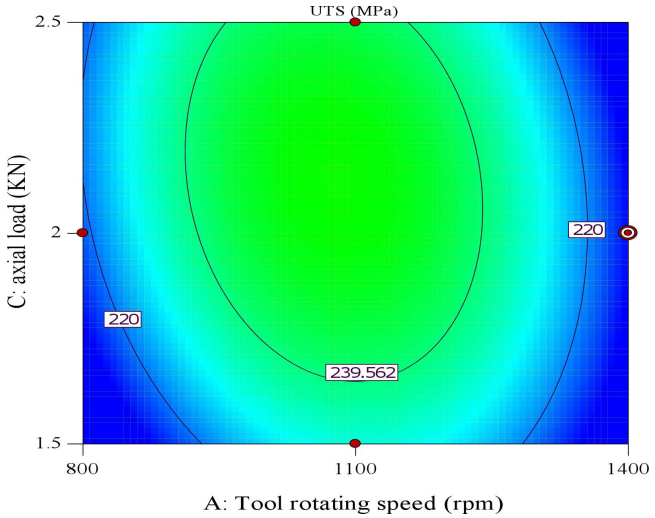

Fig. 8. Contour plots of tool rotational speed and axial load on UTS

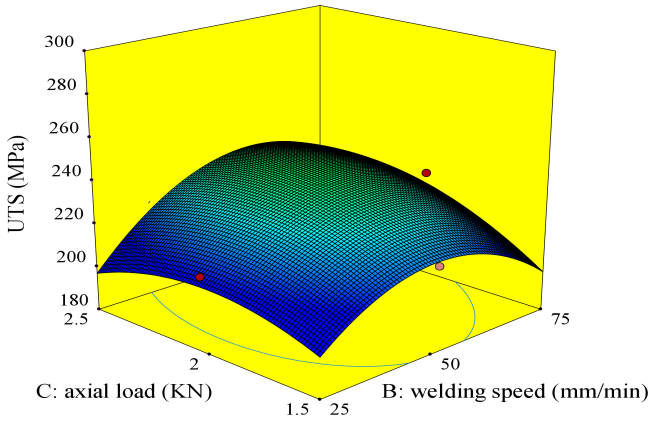

Fig. 9. Response surface graphs of axial load and welding speed on UTS

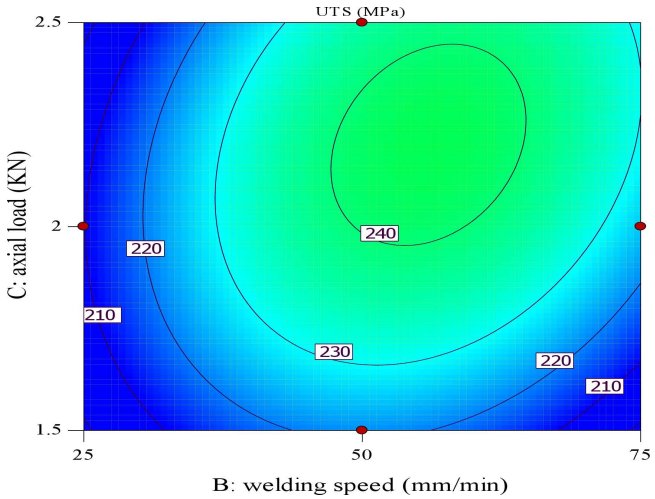

Fig. 10. Contour plots of axial load and welding speed on UTS

4. Optimizing FSW process parameters

In this work, FSW process parameters were optimized using response surface methodology (RSM). For designing a set of experiments, building a mathematical model, analyzing the optimum combination of input parameters and expressing the values graphically, RSM is the best method [12]. To achieve

the influencing temperament and an optimized condition of the process parameter on UTS, the surface plots and contour plots which are the representations of possible independence of factors have been developed for the proposed empirical relation by considering one parameter in the middle level and two parameters in the x- and y-axis as shown in Figs. 4, 6, and 8. These response contours can help in the prediction of the response (UTS) for any region of the experimental domain [15]. Figures 3, 5 and 7 show three-dimensional response surface plots for the response tensile strength obtained from the regression model. The maximum achievable UTS values have been taken from the apex of the response plot. A contour plot is created which plays a most important role in displaying the region of the optimal process visually. Creating contour plot can be more complex for second-order responses compared to the simple series of parallel lines that can occur with first-order models. Once the immobile point is found, it is usually required to characterize the response surface in the immediate vicinity of the point. Characterization involves identifying whether the immobile point is a minimum response or a maximum response or a saddle point. To categorize this, it is most undemanding to examine it through a contour plot. Influences of process parameters on UTS can be ranked [16, 17] from their respective F ratio values presented in Table 6, and provided that the degrees of freedom are same for all the input parameters. The higher F ratio value indicates that the respective term is more significant. From the F ratio values, it is concluded that rotational speed contributes more on UTS and it is followed by welding speed and axial force, for the range considered in this model. By analyzing the response surfaces and contour plots, the maximum achievable UTS value is found to be 288 MPa. The corresponding FSW parameters that yield this maximum value are tool rotational speed of 1 100 r/min, welding speed of 75 mm/min and axial force of 1.5 t.

5. Conclusions

The connections between process parameters for FS welding of AA 5083-O aluminum alloy have been secured utilizing Response Surface Methodology, which were checked for their adequacy utilizing ANOVA test and scatter diagrams, and discovered to be agreeable.

1. Response graphs and contour plots were drawn to study the effect of FSW parameters on the tensile strength of friction stir welded joints of AA 5083-O aluminium alloy.
2. The working range of optimized welding parameters for good quality FS welded joints of aluminium alloy AA 5083-O is found.

REFERENCES

[1] A.A.M. da Silva, E. Arruti, G. Janeiro, E. Aldanondo, P. Alvarez, and A. Echeverria, "Material flow and mechanical behaviour of dissimilar AA2024-T3 and AA7075-T6 aluminium alloys friction stir welds", *J. Materials and Design* 32, 2021–2027 (2011).

[2] V.-X. Tran, J. Pan, and T. Pan, "Application of Taguchi approach to optimize of FSSW parameters on joint properties of dissimilar AA2024-T3 and AA5754-H22 aluminum alloys", *Materials and Design* 51, 513–521 (2013).

[3] B. Li and Y. Shen, "A feasibility research on friction stir welding of a new-typed lap–butt joint of dissimilar Al alloys", *Materials and Design* 34, 725–731 (2012).

[4] C. Leitão, R. Louro, and D.M. Rodrigues, "Analysis of high temperature plastic behaviour and its relation with weldability in friction stir welding for aluminium alloys AA5083-H111 and A6082-T6", *Materials and Design* 37, 402–409 (2012).

[5] M. Koilraj, V. Sundareswaran, S. Vijayan, and S.R. Koteswara Rao, "Friction stir welding of dissimilar aluminum alloys AA2219 to AA5083 – optimization of process parameters using Taguchi technique", *Materials and Design* 42, 1–7 (2012).

[6] J. Grum and J.M. Slabe, "The use of factorial design and response surface methodology for fast determination of optimal heat treatment conditions of different Ni-Co-Mo surfaced layers", *J. Materials Processing Technology* 155 (30), 2026–2032 (2004).

[7] K. Manonmani, N. Murugan, and G. Buvanasekaran, "Effect of process parameters on the weld bead geometry of laser beam welded stainless steel sheets", *Int. J. Joining Materials* 17 (4), 103–109 (2005).

[8] M. Balasubramanian, V. Jayabalan, and V. Balasubramanian, "Developing mathematical models to predict tensile properties of pulsed current gas tungsten arc welded Ti-6Al-4V alloy", *Materials and Design* 29 (1), 92–97 (2008).

[9] P.K. Palani and N. Murugan, "Optimization of weld bead geometry for stainless steel claddings deposited by FCAW", *J. Materials Processing Technology* 190 (1), 291–299 (2007).

[10] P.K. Palani and N. Murugan", Sensitivity analysis for process parameters in cladding of stainless steel by flux cored arc welding", *J. Manufacturing Processes* 8 (2), 90–100 (2006).

[11] T. Hung, M. Okazaki, and K. Suzuki, "Fatigue crack propagation behavior in friction stir welding of AA6063-T5: roles of residual stress and microstructure", *Int. J. Fatigue* 43, 23–29 (2012).

[12] V. Gunaraj and N. Murugan, "Application of response surface methodology for predicting weld bead quality in submerged arc welding of pipes", *J. Material Processing Technology* 88, 266–275 (1999).

[13] J. Colligan, J. Paul, J. Konkol, J. Fisher, and P. Joseph, "Friction stir welding demonstrated for combat vehicle construction", *Welding J.* 82 (3), 1–6 (2003).

[14] K. Elangovan, V. Balasubramanian, and M. Valliappan, "Influences of tool pin profile and axial force on the formation of friction stir processing zone in AA6061 aluminium alloy", *Int. J. Advanced Manufacturing Technology* 38, 285–295 (2008).

[15] C. Tien and S.W. Lin, "Optimization of process parameters of titanium dioxide films by response surfaces methodology", *Optics Communication* 266 (2), 574–581 (2006).

[16] R. Karthikeyan and V. Balasubramanian, "Predictions of the optimized friction stir spot welding process parameters for joining AA2024 aluminum alloy using RSM", *Int. J. Advanced Manufacturing Technology* 51, 173–183 (2010).

[17] Y.C. Chen, H. Liu, and J. Feng, "Friction stir welding characteristics of different heat-treated-state 2219 aluminium alloy plates", *Material Science Engineering* A 420(1/2), 21–25 (2006).

[18] J.R. Phillip, *Taguchi Techniques for Quality Engineering*, Mc Graw-Hill, New York 1988.